Article

Ligand-Tuned Regioselectivity of a Cobalt-Catalyzed Diels#Alder Reaction. A Theoretical Study

Philipp Mo#rschel, Judith Janikowski, Gerhard Hilt, and Gernot Frenking

J. Am. Chem. Soc., **2008**, 130 (28), 8952-8966 • DOI: 10.1021/ja078242n • Publication Date (Web): 18 June 2008

JACS
ARTICLES
Published on Web 06/18/2008

Ligand-Tuned Regioselectivity of a Cobalt-Catalyzed Diels−Alder Reaction. A Theoretical Study

Philipp Mörschel, Judith Janikowski, Gerhard Hilt,* and Gernot Frenking*

Fachbereich Chemie, Philipps-Universität Marburg, D-35032 Marburg, Germany

Received October 28, 2007; E-mail: hilt@chemie.uni-marburg.de; frenking@chemie.uni-marburg.de

Abstract: Quantum chemical calculations at the BP86/def2-SVP levels of theory have been carried out for the reaction pathways of the $[Co(L)]^+$-catalyzed Diels−Alder reaction of isoprene with phenylacetylene, with L = dppe, iminA, iminB. The calculations suggest that the reactions take place in a stepwise fashion, starting with the formation of the complex $[Co(L)(isoprene)(phenylacetylene)]^+$ as precursor for the consecutive C−C bond formation. The actual Diels−Alder ring-closing reaction proceeds as an intramolecular addition of the ligands isoprene and phenylacetylene, yielding a metallacyclic intermediate after generation of the first carbon−carbon bond, which determines the regioselectivity of the reaction. There are four different conformations of the starting complexes $[Co(L)(isoprene)(phenylacetylene)]^+$ which initiate four different pathways yielding the 1,3-cyclohexadiene product. The energetically most stable conformations do not lead to the reaction pathways that have the lowest activation energies. All conformations and the associated pathways must be considered in order to obtain the kinetically most favorable reaction course. The calculated values for the regioselectivities of the $[Co(L)]^+$-catalyzed Diels−Alder reaction agree exceptionally well with the experimental values. The calculations concur with the experimental finding that the *para* product is kinetically favored for L = dppe while the formation of the *meta* product is kinetically favored when L = iminA or iminB. The different regioselectivies for L = dppe and L = iminA or iminB come from (a) the steric interactions of the bidentate ligands with the isoprene and phenylacetylene moieties in $[Co(L)(isoprene)(phenylacetylene)]^+$, which determine the distance between the carbon atoms forming the C−C bond, and (b) the relative energies of the different starting complexes. The first C−C bond formed in the rate-determing step of the $[Co(dppe)]^+$-catalyzed reaction yielding the *para* product is the C4−C1′ bond, and for the *meta* product it is the C1−C1′ bond. The opposite order is found for the $[Co(iminA)]^+$- and $[Co(iminB)]^+$-catalyzed reactions, where the C1−C2′ bond formation is the initial step toward the *para* product, while the C4−C2′ bond is first formed in the reaction yielding the *meta* product. The calculations suggest that a less polar solvent should reduce the preference for formation of the *meta* product in the $[Co(iminA)]^+$- and $[Co(iminB)]^+$-catalyzed reactions but would enhance the formation of the *para* product in the $[Co(dppe)]^+$-catalyzed reaction. Experimental tests using toluene as solvent instead of dichloromethane confirm the theoretical predictions.

Introduction

The explanation and prediction of the stereoselectivity of pericyclic reactions with the help of molecular orbital theory is one of the greatest success stories in theoretical organic chemistry.[1] The introduction of frontier orbital theory[2] and the Woodward−Hoffmann rules[3] solved the mystery about the reaction mechanism of cycloaddition reactions and molecular rearrangements, which were shown to be governed by the symmetry of molecular orbitals.[1,4] The reaction course of pericyclic reactions in terms of orbital interactions has become a standard model in modern organic chemistry textbooks.[5] For example, the addition of a substituted alkene or alkyne to a 2-substituted diene may lead to two different regioisomers, as shown in Scheme 1. According to the Woodward−Hoffmann rule, the formation of the *para* product is in most cases favored

Scheme 1. Diels−Alder Reaction between an Alkyne and a 1,3-Diene Leading to the *Para* and *Meta* Products

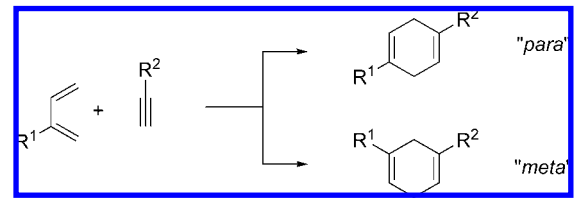

(1) (a) Fleming, I. *Frontier Orbitals and Organic Chemical Reactions*; Wiley: New York, 1976. (b) Gilchrist, T. L.; Storr, R. C. *Organic reactions and orbital symmetry*, 2nd ed.; Cambridge University Press: Cambridge, 1971.
(2) (a) Fukui, K. *Acc. Chem. Res.* **1971**, *4*, 57. (b) Fukui, K. *Theory of Orientation and Stereoselection*; Springer Verlag: Berlin, 1975.
(3) Woodward, R. B.; Hoffmann, R. *The Conservation of Orbital Symmetry*; Verlag Chemie: Weinheim, 1970.
(4) (a) Houk, K. N. *Acc. Chem. Res.* **1975**, *8*, 361. (b) Sustmann, R. *Pure Appl. Chem.* **1974**, *40*, 569.
(5) (a) Vollhardt, K. P. C.; Schore, N. E. *Organic Chemistry: Structure and Function*, 5th ed.; W. H. Freeman: New York, 2007. (b) Smith, M. B.; March, J. *March's Advanced Organic Chemistry*, 6th ed.; Wiley: New York, 2007.

10.1021/ja078242n CCC: $40.75

over the *meta* product,[6] which is explained on the basis of the polarization of the frontier molecular orbitals (FMOs).[1] The development of chemical reactions that lead to *meta* products is therefore a challenge for synthetic chemistry.

It is well known that the reactivity and stereoselectivity of pericyclic reactions can be strongly influenced by Lewis acids, which may have a distinct stereoelectronic effect on the reaction path.[7] In particular, transition metal complexes may impact the observed stereoselectivity and the reaction rate of concerted reactions such as the Diels−Alder cycloaddition reaction.[8] It is not easy to explain the particular influence of the metal catalyst on the reaction course, because the outcome of the reaction is often dictated by a subtle interplay between electronic and steric factors which makes it difficult to interpret the observed reactivity. Quantum chemical calculations can be helpful for the purpose, but quantitative studies of reaction mechanisms are not trivial because the energy differences between competing pathways that lead to different isomers are often very small and the investigated molecules are usually quite large. A pertinent example is the density functional theory (DFT) study of the endo selectivity in the Diels−Alder reaction of cyclopentadiene with acrylate imide in the presence of bis(oxazoline)-Cu(II) Lewis acid catalysts, which was recently reported by Evanseck and co-workers.[9] The authors showed that it is the unique positioning of the substituent at the C_2 position of the bis(oxazoline) ligand that determines the stereospecific pathway and the enhanced rate of the reaction. There are two noteworthy aspects of the carefully executed work of Evanseck et al.:[9] (1) the relative energies of the transition states for the exo and endo products were in agreement with experimental observations only when solvent effects were included in the calculations, and (2) the transition states for the metal-catalyzed addition of cyclopentadiene to acrylate imide indicate a concerted pathway like in the uncatalyzed reaction where both C−C bonds are formed in a single step.

In recent experimental work, one of us reported on the Diels−Alder reaction of the diene components isoprene and other 2-substituted 1,3-butadienes with terminal alkynes (Scheme 2) in the presence of a cobalt complex with the general formula $[CoBr_2(L)]$.[10] The surprising finding was that, depending on the choice of the ligand L, the reaction may either dominantly yield the *para* product (which, according to the frontier orbital theory, is the favored product of the uncatalyzed reaction)[1] or mainly give the *meta* product. For example, while the reaction between isoprene and phenylacetylene using $[CoBr_2(dppe)]$ (dppe = 1,2-bis(diphenylphosphanyl)ethane) gives a *meta*:*para* ratio of 15:85, changing the ligand L to an imine ($[CoBr_2(imin)]$) gives for the same reaction a *meta*:*para* ratio of 99:1 when iminA is used and a ratio 95:5 when iminB is employed (Scheme 2).[10] It is important to know that the high yields and high ratio are observed only when the reactions are carried out in the presence of zinc powder and ZnI_2. To explain the latter finding, it was postulated that the neutral Co(II) complex is reduced in situ to the Co(I) complex and the remaining halide is abstracted by the Lewis acid to generate the cationic $[Co(L)]^+$ complex which was suggested as the catalytically active species. The mechanism of the cobalt-catalyzed Diels−Alder reaction shown in Scheme 2 and an explanation for the change in the *meta*:*para* regioselectivity could not be given at that point.

Scheme 2. Experimentally Observed[10] Regioselectivity of the Cobalt-Catalyzed Diels−Alder Reaction of Phenylacetylene and Isoprene

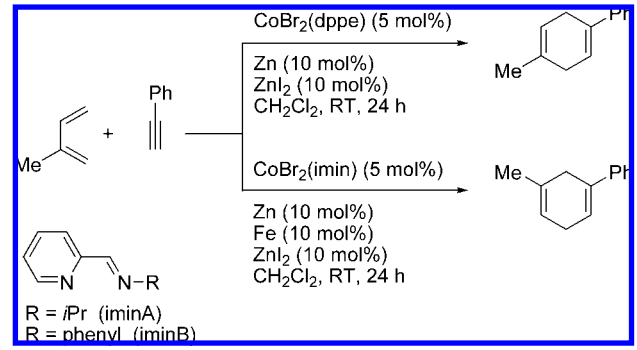

The experimentally observed ligand-tuning of the regioselectivity of the Diels−Alder reaction opens new pathways for the synthesis of a large variety of organic compounds. In order to explore the mechanism of the reaction and to understand the origin of the strong ligand effect on the *meta*:*para* selectivity, we carried out an exhaustive theoretical investigation of the reaction pathways using gradient-corrected DFT methods. We optimized the geometries and transition states for the uncatalyzed and for the metal-catalyzed Diels−Alder reaction with isoprene as diene and with phenylacetylene as the dienophile component. The chosen cobalt complexes are $[Co(dppe)]^+$, $[Co(iminA)]^+$, and $[Co(iminB)]^+$ (see Scheme 2 for the ligands). Energy calculations at the stationary points were carried out with inclusion of thermal and entropic contributions. We also estimated the effect of the solvent CH_2Cl_2 that was used in the experiments[10] with a polarizable continuum model (PCM).[11]

Methods

Geometry optimizations without symmetry constraints were carried out using the Gaussian03 optimizer[12] together with TurboMole[13] energies and gradients at the BP86[14]/def2-SVP[15] level of theory. For the phenyl rings, a minimal basis set was used (benzene BS), except for the α-C atom. Stationary points were characterized as minima (number of imaginary frequencies $i = 0$) or as transition states ($i = 1$) by calculating the Hessian matrix analytically at this

(6) Throughout this paper, the terms *para* and *meta* are used synonymously for the 1,4-disubstituted 1,4-cyclohexadienes and 2,4-disubstituted 1,4-cyclohexadienes, respectively.
(7) (a) Evans, D. A.; Johnson, J. S. In *Comprehensive Asymmetric Catalysis*; Jacobsen, E. N., Pfaltz, A., Yamamoto, H., Eds.; Springer: New York, 1999; Vol. 3, pp 1178−1235, and references therein. (b) Ghosh, A. K.; Mathivanan, P.; Cappiello, J. *Tetrahedron: Asymmetry* **1998**, *9*, 1–45. (c) Jørgensen, K. A. *Angew. Chem., Int. Ed.* **2000**, *39*, 3558–3588. (d) Johnson, J. S.; Evans, D. A. *Acc. Chem. Res.* **2000**, *33*, 325–335. (e) Corey, E. J.; Ishinhara, K. *Tetrahedron Lett.* **1992**, *33*, 6807–6810. (f) Bolm, C.; Martin, M.; Simic, O.; Verrucci, M. *Org. Lett.* **2003**, *5*, 427–429. (g) Rechavi, D.; Lemaire, M. *Chem. Rev.* **2002**, *102*, 3467–3494.
(8) *Transition Metals for Organic Synthesis*, 2nd ed.; Beller, M., Bolm, C., Eds.; Wiley-VCH: Weinheim, 2004.
(9) DeChancie, J.; Acevedo, O.; Evanseck, J. D. *J. Am. Chem. Soc.* **2004**, *126*, 6043.
(10) (a) Hilt, G.; Janikowski, J.; Hess, W. *Angew. Chem.* **2006**, *118*, 5328. (b) Hilt, G.; Janikowski, J.; Hess, W. *Angew. Chem., Int. Ed.* **2006**, *45*, 5204.
(11) (a) Tomasi, J.; Persoci, M. *Chem. Rev.* **1994**, *94*, 2027. (b) Cossi, M.; Cammi, R.; Thomas, J.; Barone, V. *Chem. Phys. Lett.* **1996**, *255*, 327.
(12) Frisch, M. J.; et al. *Gaussian03*; Gaussian, Inc.: Pittsburgh, PA, 2003.
(13) Ahlrichs, R.; Baer, M.; Haeser, M.; Horn, H.; Koelmel, C. *Chem. Phys. Lett.* **1989**, *162*, 165.
(14) (a) Becke, A. D. *Phys. Rev. A* **1988**, *38*, 3098. (b) Perdew, J. P. *Phys. Rev. B* **1986**, *33*, 8822.
(15) Schaefer, A.; Horn, H.; Ahlrichs, R. *J. Chem. Phys.* **1992**, *97*, 2571.

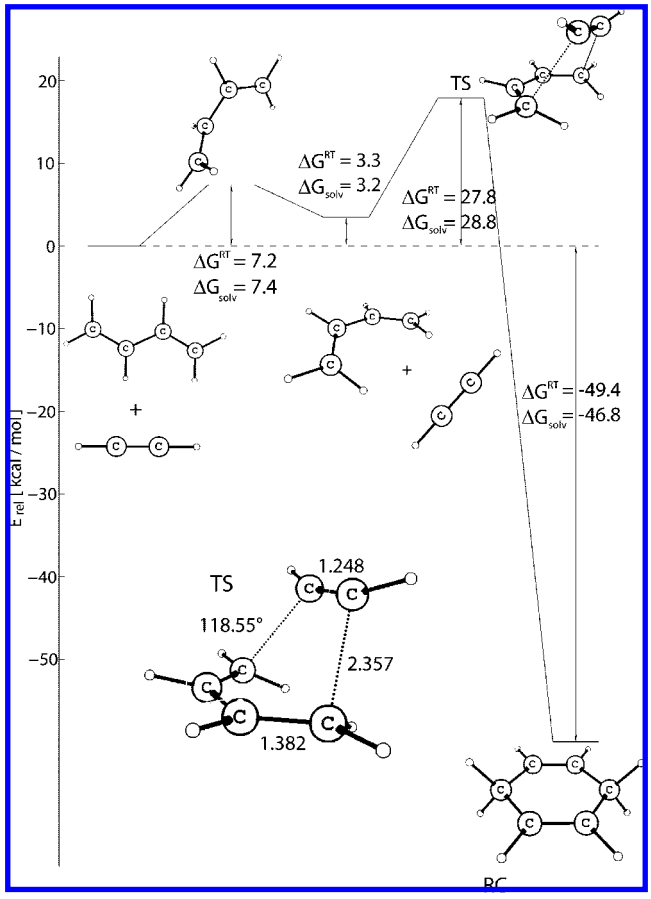

Figure 1. Calculated (BP86/def2-SVP) reaction course for the addition of acetylene to 1,3-butadiene. Free energy difference at 298 K (ΔG^{RT}) and after considering solvent effects of CH_2Cl_2 (ΔG_{solv}). The calculated interatomic distances are given in angstroms. Note that the reference value for the energies at 0 kcal/mol refers to the ΔG_{solv} scale.

level.[16] Thermodynamic corrections were taken from these calculations. The standard state for all thermodynamic data is 298.15 K and 1 atm. For the BP86/def2-SVP calculations, the resolution-of-identity (RI) method was applied.[17] All-electron basis sets were used for all atoms with the exception of cobalt, where a small-core effective core potential approximation was applied.[18] The solvent effect on the calculated energies was estimated with a PCM.[11] The latter calculations were carried out with a dielectricity constant $\epsilon = 8.93$ for the solvent CH_2Cl_2 used in the experiments.[10]

Uncatalyzed Reactions. We first calculated the reaction path for the uncatalyzed addition of the parent compounds 1,3-butadiene and acetylene at the same BP86/def2-SVP level of theory which could be afforded for the larger systems. The calculated data are helpful because they can be compared with previous high-level calculations using correlated ab initio methods.[19] The theoretically predicted reaction profile is shown in Figure 1. The most important interatomic distances are also displayed. The complete set of geometries and energies of all calculated species in this work is given as Supporting Information. Note that the reference value for the energies at 0 kcal/mol in Figure 1 and the following figures that show reaction profiles refers to the ΔG_{solv} scale.

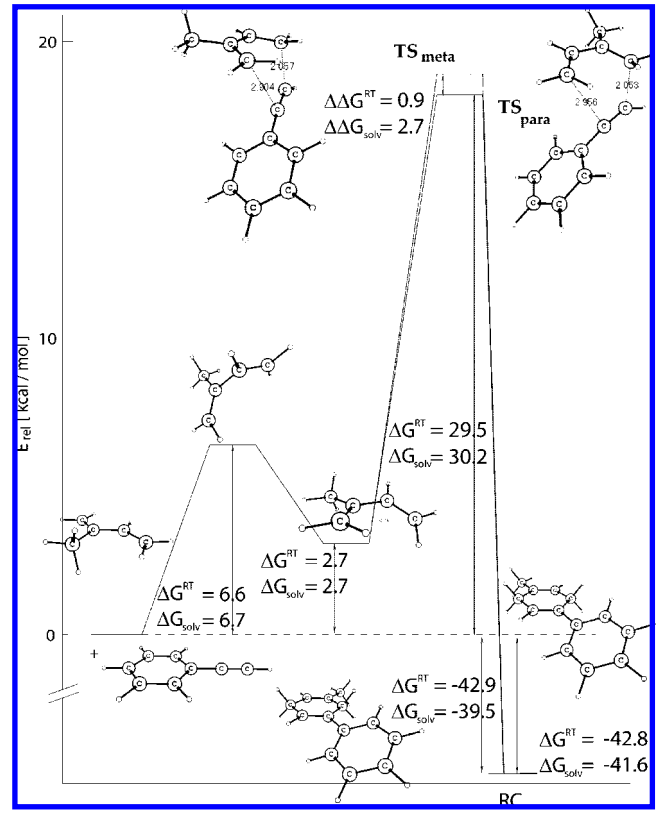

Figure 2. Calculated (BP86/def2-SVP) reaction course for the addition of phenylacetylene to isoprene. Free energy difference at 298 K (ΔG^{RT}) and after considering solvent effects of CH_2Cl_2 (ΔG_{solv}). The calculated interatomic distances are given in angstroms. Note that the reference value for the energies at 0 kcal/mol refers to the ΔG_{solv} scale.

The calculations suggest that the *trans* form of 1,3-butadiene first rearranges to the twisted *cis* form, which is 3.3 kcal/mol higher in energy than the *trans* form at room temperature. The calculated transition state for the perfectly concerted [4+2] addition of acetylene gives an overall activation barrier at room temperature of $\Delta G^{\ddagger}_{RT} = 27.8$ kcal/mol. The inclusion of the solvent effect induced by dichloromethane increases the barrier to $\Delta G^{\ddagger}_{solv} = 28.8$ kcal/mol. The optimized transition state has C_s symmetry, with both newly formed C−C bonds having equal distances of 2.357 Å (Figure 1). The BP86/def2-SVP calculations suggest that the reaction is exergonic by $\Delta G_{RT} = -49.4$ kcal/mol. Previous ab initio calculations, which did not consider entropic or solvent effects, predicted at the highest level employed in that work (G2MS) that the reaction at 0 K has a barrier of 25.8 kcal/mol and that it is exothermic by −52.2 kcal/mol.[19] The latter values may be compared with the present BP86/def2-SVP calculations, which give $\Delta E^{\ddagger}_{ZPE} = 17.9$ kcal/mol and $\Delta E_{ZPE} = -60.0$ kcal/mol. Our calculations thus give activation barriers that are a bit too low and reaction energies that are slightly too exothermic. This is not a reason for great concern since we are interested in the *differences* between the energies of transition states and energy minima of competing reaction pathways. It can reasonably be assumed that the errors in the absolute values cancel to a large degree.

Next we calculated the reaction paths for the uncatalyzed addition of isoprene to phenylacetylene yielding the *meta* and *para* products. The most important results are shown in Figure 2. The calculations suggest that the reaction of the substituted compounds has a slightly higher barrier and that it is less exothermic/exergonic than the addition of the parent system. The formation of the *para* product is kinetically favored over the formation of the *meta* product ($\Delta\Delta G^{\ddagger}_{RT} = 0.9$ kcal/mol), but the two isomers are thermodynamically nearly degenerate at room temperature, with $\Delta\Delta G_{RT} = 0.1$ kcal/mol in favor of the *meta* product. Note that the inclusion of

(16) Deglmann, P.; Furche, F.; Ahlrichs, R. *Chem. Phys. Lett.* **2002**, *362*, 511.
(17) (a) Eichkorn, K.; Treutler, O.; Ohm, M.; Häser, M.; Ahlrichs, R. *Chem. Phys. Lett.* **1995**, *242*, 652. (b) Weigend, F. *PhysChemChemPhys* **2006**, *8*, 1057.
(18) Hay, P. J.; Wadt, W. R. *J. Chem. Phys.* **1985**, *82*, 299.
(19) Froese, R. D.; West, S. C.; Morokuma, K.; Coxon, J. M. *J. Org. Chem.* **1997**, *62*, 6991.

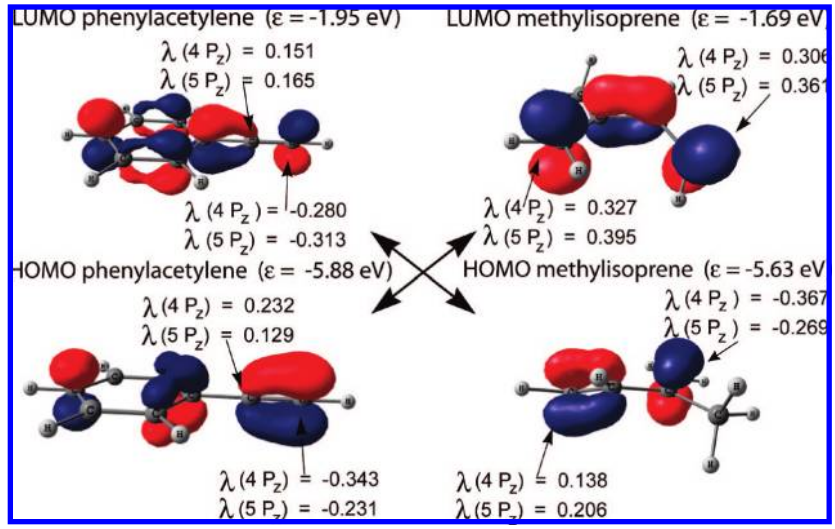

Figure 3. Shape of the frontier orbitals of phenylacetylene and isoprene. Eigenvalues of the HOMO and LUMO (eV) and atomic orbital coefficients at the carbon atoms that form the C−C bonds. Calculated at BP86/def2-SVP.

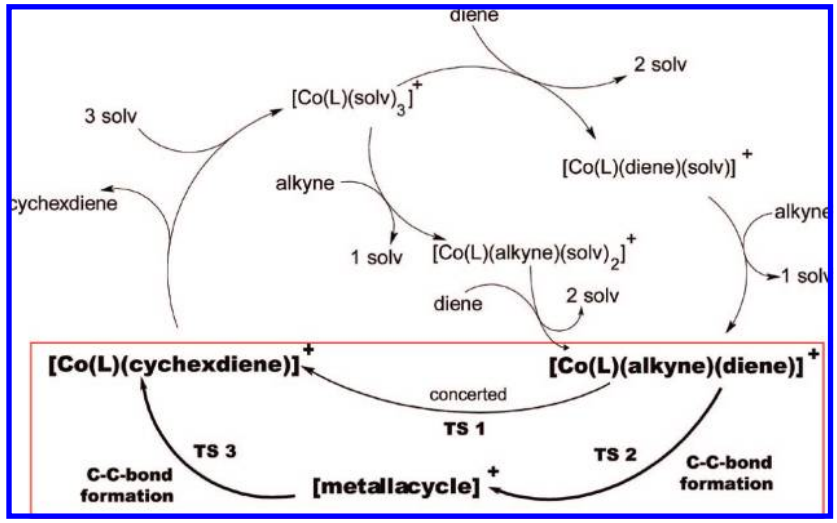

Figure 4. Postulated catalytic cycle for the $[Co(L)]^+$-catalyzed Diels−Alder reaction of alkynes and dienes, which was studied experimentally by Hilt et al.[10] The reaction steps in the red box have been calculated.

the solvent effect induced by dichloromethane enhances the preference for the formation of the *para* product. The kinetic discrimination increases to $\Delta\Delta G^{\ddagger}_{solv} = 2.7$ kcal/mol, and the *para* product becomes 2.1 kcal/mol lower in energy than the *meta* product. We want to point out that, in both transition states leading to the *para* and to the *meta* product, phenylacetylene approaches isoprene first with the terminal carbon atom where the nascent carbon−carbon bond is already much shorter compared with the developing C−C bond of the internal carbon atom.

The lower activation barrier for the *para* product is in agreement with the prediction of the FMO theory and the Woodward−Hoffmann rules.[1,3] The calculated orbital energies of isoprene and phenylacetylene indicate that the reaction falls into the category of Diels−Alder reactions with normal electron demand; i.e., the dominating interaction takes place between the HOMO of isoprene and the LUMO of phenylacetylene. Figure 3 shows the frontier orbitals of the two molecules. According to the frontier orbital theory, the atom with the largest coefficient of the HOMO of isoprene binds to the atom with the largest coefficient of the LUMO of phenylacetylene.[1] Figure 3 shows that the calculated coefficients are in agreement with the lower energy for the transition state yielding the *para* product.

Catalyzed Reactions. On the basis of the experimental observations, we postulate the catalytic cycle shown in Figure 4 for the cobalt-catalyzed Diels−Alder reaction between isoprene and phenylacetylene. It is suggested that the initial $[CoBr_2(L)]$ complex is reduced to $[Co(L)]^+$, which enters the catalytic cycle after binding three solvent molecules (Solv) in the diamagnetic 18-electron complex $[Co(L)(Solv)_3]^+$. The optimized geometries of the latter complex with the solvent molecule CH_2Cl_2 and the three ligands L = dppe, iminA, and iminB are shown in Figure 5. Methylene chloride was used as the solvent in the experimental work.[10] We searched for other conformations of the solvent molecules in $[Co(L)(Solv)_3]^+$ and found numerous low-lying energy minima. The structures shown in Figure 5 are the lowest-energy structures.

In the catalytic cycle shown in Figure 4, the solvent ligands are substituted by the bidentate diene and monodentate alkyne substrate molecules, yielding the adduct $[Co(L)(diene)(alkyne)]^+$. The latter complex is the starting compound for the Diels−Alder reaction that leads to the coordinatively unsaturated cyclohexadiene complex $[Co(L)(cyclohexadiene)]^+$. This reaction step may occur in a concerted fashion via TS1 or as a two-step process via TS2 and TS3. After releasing the cyclohexadiene product molecule, the catalytically active species $[Co(L)]^+$ starts a new

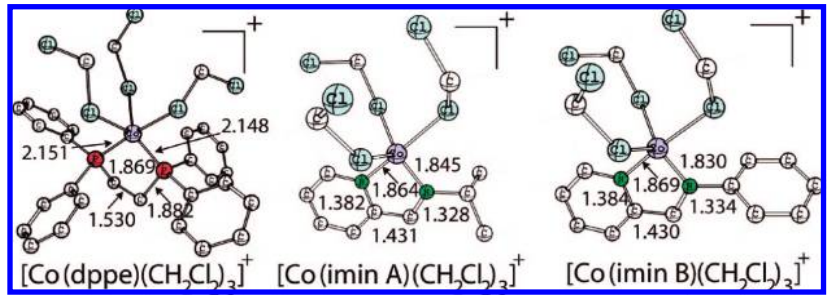

Figure 5. Optimized structures (BP86/def2-SVP) of the complexes $[Co(dppe)(CH_2Cl_2)_3]^+$, $[Co(iminA)(CH_2Cl_2)_3]^+$, and $[Co(iminB)(CH_2Cl_2)_3]^+$. The calculated interatomic distances are given in angstroms. Hydrogen atoms are omitted for clarity.

catalytic cycle, either by adding first the solvent molecules, yielding $[Co(L)(solv)_3]^+$ which are then substituted, or by directly binding new substrate molecules. Hence, we identify the reactions from $[Co(L)\ (diene)(alkyne)]^+$ to $[Co(L)(cyclohexadiene)]^+$ as the crucial steps which have been calculated and analyzed for diene = isoprene and alkyne = phenylacetylene in order to understand the difference between the regioselectivity of L = dppe and L = imin. Although it cannot be totally excluded that the reaction takes place without prior complexation of either reaction partners, we think that this is unlikely because the binding energies of isoprene and phenylacetylene are clearly higher than those of the solvent molecules CH_2Cl_2. Unlike the theoretical study by Evanseck and co-workers[9] of the Diels−Alder reaction of cyclopentadiene with acrylate imide in the presence of $[Cu(L)]^{2+}$, where the bulky bisoxazoline ligand L prevents the coordination of the reacting molecules at the metal, the calculations showed that the dppe and imin ligands in $[Co(L)]^+$ easily tolerate the further complexation with isoprene and phenylacetylene as ligands.

Cobalt-Catalyzed Reaction of 1,3-Butadiene with Acetylene. In order to investigate the influence of the cobalt catalyst on the reaction course of the Diels−Alder reaction, we first calculated the reaction profiles for the addition of the parent compounds 1,3-butadiene and acetylene at the BP86/def2-SVP level of theory in the presence of $[Co(L)]^+$, where L = dppe, iminA, and iminB:

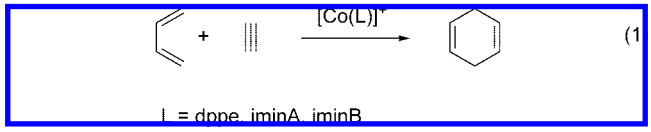

An extensive search for conformations of the precursor complexes for reaction 1, $[Co(L)(1,3\text{-butadiene})(acetylene)]^+$, gave two energy minima when L = dppe and four minima when L = iminA or iminB, which are the starting points for two and four different reaction pathways of the different catalysts, respectively. Figure 6 displays the calculated reaction profiles for reaction 1 with $[Co(dppe)]^+$ as catalyst.

The reaction path A1 shown in Figure 6a starts with the energetically lower-lying conformation of $[Co(dppe)(1,3\text{-butadiene})(acetylene)]^+$ (**1a**), which reacts with an energy barrier of $\Delta G^{\ddagger}_{solv} = 16.1$ kcal/mol, yielding the metallacyclic complex **1b**. Note that only one C−C bond is formed during the reaction **1a** → **1b**, which is exergonic by $\Delta G_{solv} = -16.6$ kcal/mol. Compound **1b** first rearranges with a barrier of $\Delta G^{\ddagger}_{solv} = 17.2$ kcal/mol via **TS1b** to form the intermediate **1c**, from which the second C−C bond forms, yielding complex **1d** in an exergonic step. The latter reaction has only a very small barrier of $\Delta G^{\ddagger}_{solv} = 1.3$ kcal/mol. The overall reaction A1 is strongly exergonic, with $\Delta G_{solv} = -36.1$ kcal/mol. The rate-determining step is the entrance reaction **1a** → **1b**, which has a barrier of $\Delta G^{\ddagger}_{solv} = 16.1$ kcal/mol. Note that the solvent effect slightly increases the barrier by 0.8 kcal/mol.

Figure 6b displays the alternative reaction course A2, which starts with the energetically higher-lying isomer **1a′**, which is $\Delta G_{solv} =$ 5.1 kcal/mol less stable than **1a**. Reaction path A2 is kinetically favored over reaction path A1, in spite of the higher-lying starting point. The former reaction pathway leads in a single step to the same intermediate **1c** that is formed in a two-step reaction in pathway A1. The activation barrier for the reaction path A2, **1a′** → **1c**, is only $\Delta G^{\ddagger}_{solv} = 3.4$ kcal/mol. The total activation barrier of A2, which includes the energy difference between **1a** and **1a′** ($\Delta G_{solv} = 5.1$ kcal/mol), is thus only $\Delta G^{\ddagger}_{solv} = 8.5$ kcal/mol. The latter value is smaller than the rate-determining activation barrier of reaction course A1 ($\Delta G^{\ddagger}_{solv} = 16.1$ kcal/mol). The calculations suggest that the $[Co(dppe)]^+$-catalyzed Diels−Alder reaction of 1,3-butadiene and acetylene is a stepwise process in which the two C−C bonds are formed in consecutive steps via the intermediate **1c**. Reaction pathway A1 is a three-step reaction that requires a rearrangement of the initially formed intermediate **1b** → **1c**, while the more favorable pathway A2 is a two-step reaction in which the two C−C bonds are formed in each step. The activation barrier for the formation of the second C−C bond is very small, however.

The four calculated reaction courses, B1−B4, for the addition of 1,3-butadiene to acetylene in the presence of $[Co(iminA)]^+$ are shown in Figure 7. There are now four pathways instead of two because the two donor sites of ligand iminA are different, while the donor sites of dppe are the same. The reaction course B1 starts with the energetically lowest-lying conformation of $[Co(iminA)(1,3\text{-butadiene})(acetylene)]^+$ (**2a**), where in the initial reaction one C−C bond is formed, yielding the metallacyclic compound **2b**. The activation barrier for the exergonic ($\Delta G_{solv} = -16.2$ kcal/mol) reaction **2a** → **2b** is $\Delta G^{\ddagger}_{solv} = 16.7$ kcal/mol, which makes this the rate-determining step of the reaction course B1. The metallacycle **2b** rearranges to the intermediate **2c**, which is the precursor species for the formation of the second C−C bond yielding the product complex **2d**. We could not locate a transition state for the rearrangment **2b** → **2c** because the potential energy surface (PES) is very shallow in the vicinity of the energy minimum **2c**. We think that the barrier for the rearrangement is very small and that it is not relevant for the reaction. The overall reaction course B1, which involves three steps (Figure 7a), thus looks very similar to the reaction path A1 (Figure 6a).

A very similar profile is also found for the reaction course B2 (Figure 7b), which opens with structure **2a′**. The latter complex is $\Delta G_{solv} = 0.7$ kcal/mol less stable than **2a**. In **2a′**, the butadiene ligand is oriented toward the pyridine ring and the acetylene ligand is oriented toward the imino group. The formation of the first C−C bond first takes place at the imino site of the complex (see **TS2a′**). The metallacyclic moiety rotates during the reaction, yielding **2b′**, where the fully developed C−C bond is found at the pyridine site while the second C−C bond is formed at the imino site (cf. **TS2c′**). A comparison of reaction path B1 (Figure 7a) with B2 (Figure 7b) shows that, in the former reaction course, the formation of both C−C bonds takes place at the pyridine site instead of the imine site. The activation barrier for the rate-determining step **2a′** → **2b′** of reaction path B2 ($\Delta G^{\ddagger}_{solv} = 15.2$ kcal/mol) is slightly lower than that for reaction path B1 ($\Delta G^{\ddagger}_{solv} = 16.7$ kcal/mol). Since the former path opens with starting complex **2a′**, which is $\Delta G_{solv} =$

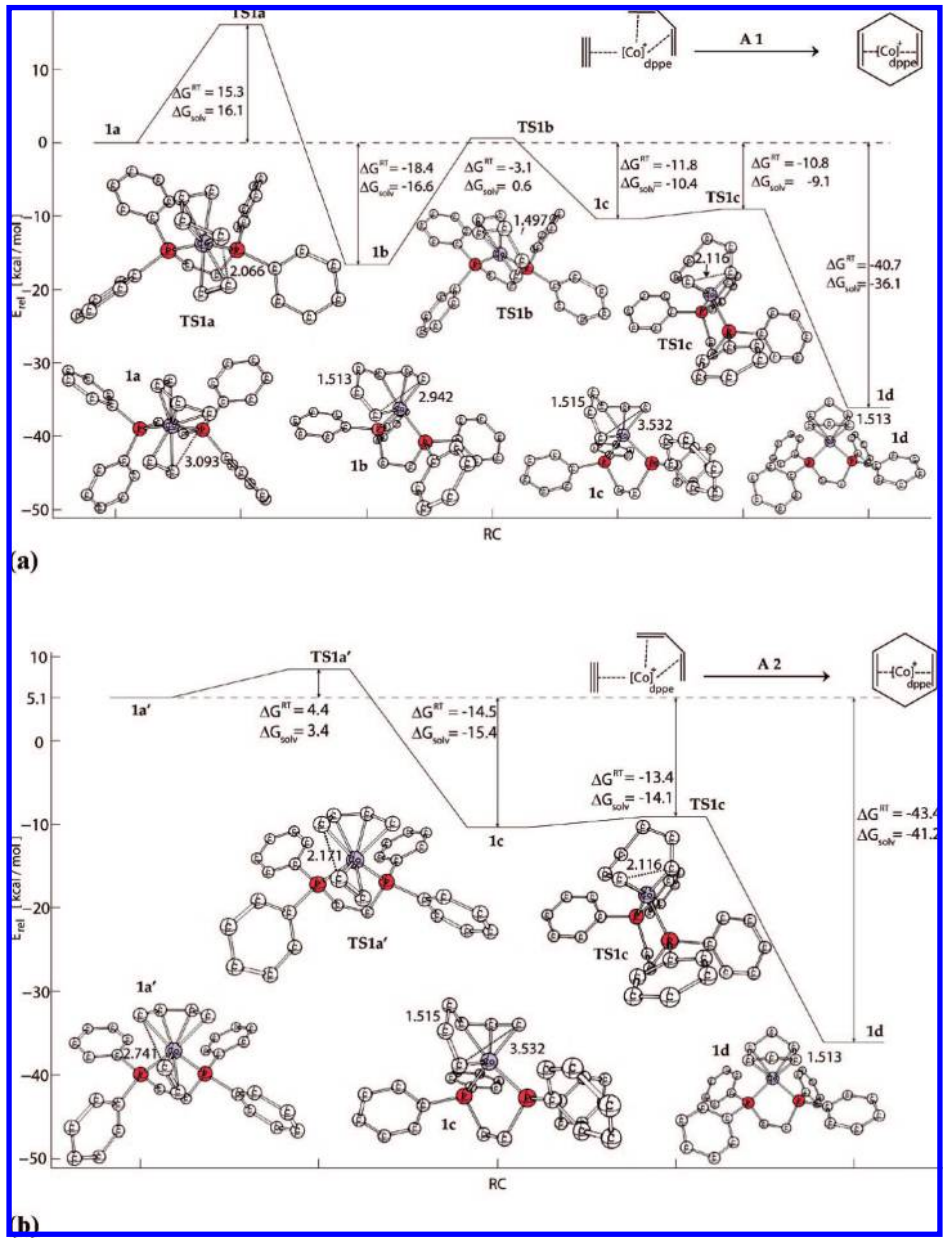

Figure 6. Calculated (BP86/def2-SVP) reaction courses A1 and A2 for the addition of acetylene to 1,3-butadiene catalyzed by $[Co(dppe)]^+$. Free energy difference at 298 K (ΔG^{RT}) and after considering solvent effects of CH_2Cl_2 (ΔG_{solv}). The calculated interatomic distances are given in angstroms. Note that the reference value for the energies at 0 kcal/mol refers to the ΔG_{solv} scale. Hydrogen atoms are omitted for clarity.

0.7 kcal/mol higher in energy than **2a**, reaction path B2 has an overall activation energy that is $\Delta\Delta G^{\ddagger}_{solv} = 0.9$ kcal/mol lower than that of B1.

The alternative reaction courses, B3 (Figure 7c) and B4 (Figure 7d), open with the starting complexes **2a″** and **2a‴**, which are slightly higher in energy than **2a**, but the activation barriers are clearly smaller than for reactions B1 and B2. Unlike the latter processes, B3 and B4 are two-step reactions that resemble reaction path A2 with a single intermediate, while B1 and B2 have two intermediates. There is no rearrangement of the metallacyclic intermediates in B3 and B4, because the initial reactions, where the first C−C bonds are formed, directly give the precursor species for the formation of the second C−C bond. In B3, the first C−C bond is formed in the reaction **2a″** → **2c**, yielding in a two-step process the same intermediate as in reaction course B1 (Figure 7a). The activation barrier for the reaction **2a″** → **2c** is only $\Delta G^{\ddagger}_{solv} =$ 6.7 kcal/mol. The overall activation barrier for B3 is thus $\Delta G^{\ddagger}_{solv}$ = 8.1 kcal/mol because **2a″** is 1.4 kcal/mol higher in energy than **2a**. The same value is calculated for the reaction course B4. The activation barriers for both pathways **2a″** → **2c** and **2a‴** → **2c′** are $\Delta G^{\ddagger}_{solv} = 8.1$ kcal/mol. The three-step pathways B1 and B2 are predicted to be kinetically much less favorable than the two-step pathways B3 and B4. Note that, in reaction course B3, the first C−C bond is formed at the imino site, while the second C−C bond is formed at the pyridine site. The converse sequence is found for reaction course B4, where the first C−C bond is formed at the pyridine site, while the second C−C bond is formed at the imino site.

We also calculated the reaction profiles C1−C4 for the addition of 1,3-butadiene to acetylene in the presence of $[Co(iminB)]^+$, which has a phenyl substituent at the imino group instead of the isopropyl group in iminA (Scheme 2). The calculated reaction profiles C1−C4 for the $[Co(iminB)]^+$-catalyzed Diels−Alder reaction are very similar to the reaction courses B1−B4 for the $[Co(iminA)]^+$-catalyzed reaction; therefore, they are not shown here. The theoretically predicted reaction pathways C1−C4 are shown in Figure S1 (Supporting Information). Here we give in Figure 8

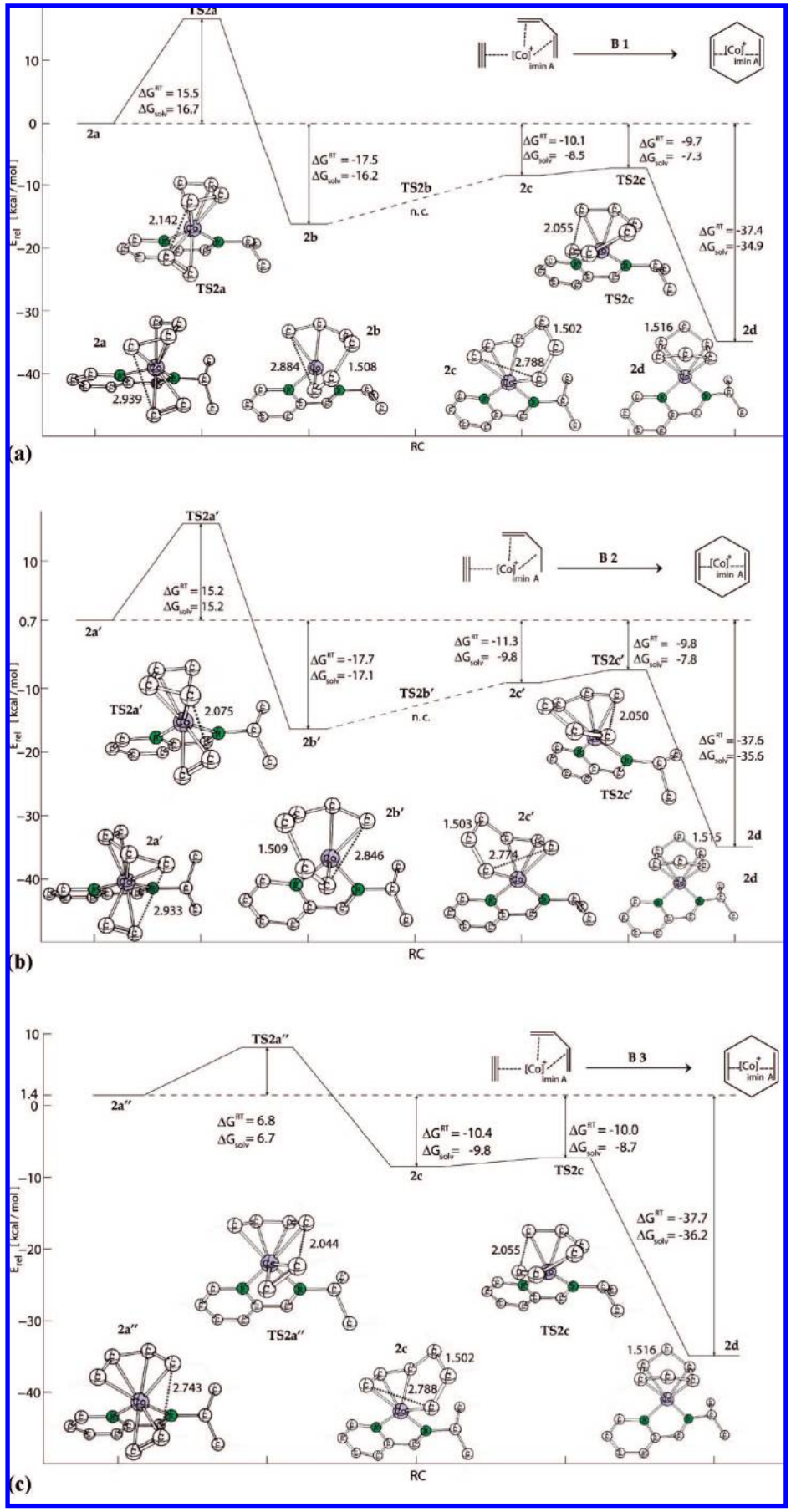
TS2a
B 1
[Co]
imin A
ΔG^RT = 15.5
ΔG_solv = 16.7
2a
ΔG^RT = -17.5
ΔG_solv = -16.2
2b
TS2b
n.c.
ΔG^RT = -10.1
ΔG_solv = -8.5
2c
TS2c
ΔG^RT = -9.7
ΔG_solv = -7.3
ΔG^RT = -37.4
ΔG_solv = -34.9
2d
E_rel [kcal/mol]
RC
(a)
TS2a′
B 2
ΔG^RT = 15.2
ΔG_solv = 15.2
2a′
ΔG^RT = -17.7
ΔG_solv = -17.1
2b′
TS2b′
n.c.
ΔG^RT = -11.3
ΔG_solv = -9.8
2c′
TS2c′
ΔG^RT = -9.8
ΔG_solv = -7.8
ΔG^RT = -37.6
ΔG_solv = -35.6
(b)
TS2a″
B 3
2a″
ΔG^RT = 6.8
ΔG_solv = 6.7
ΔG^RT = -10.4
ΔG_solv = -9.8
ΔG^RT = -10.0
ΔG_solv = -8.7
ΔG^RT = -37.7
ΔG_solv = -36.2
(c)

Figure 7

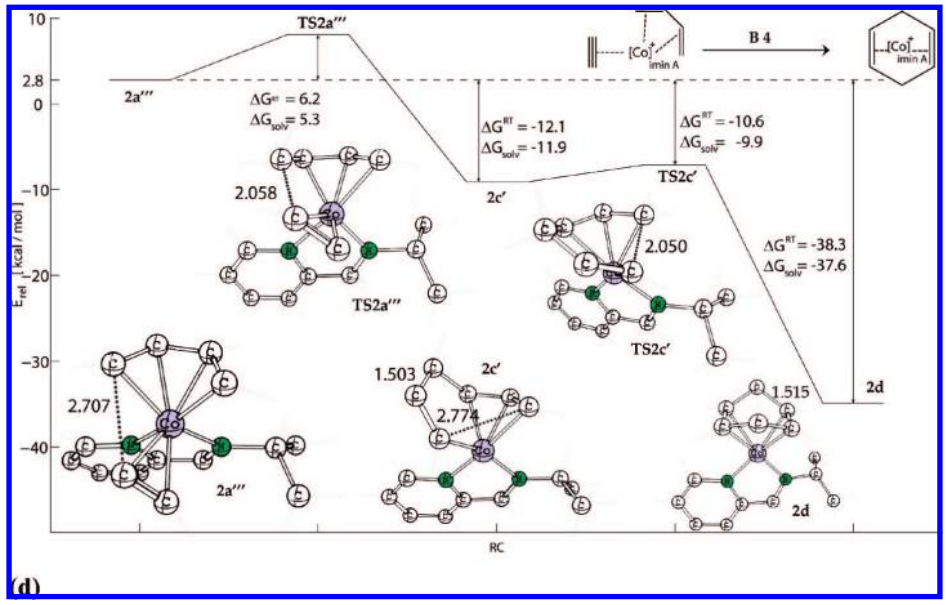

Figure 7. Calculated (BP86/def2-SVP) reaction courses B1−B4 for the addition of acetylene to 1,3-butadiene catalyzed by $[Co(iminA)]^+$. Free energy difference at 298 K (ΔG^{RT}) and after considering solvent effects of CH_2Cl_2 (ΔG_{solv}). The calculated interatomic distances are given in angstroms. Note that the reference value for the energies at 0 kcal/mol refers to the ΔG_{solv} scale. Hydrogen atoms are omitted for clarity.

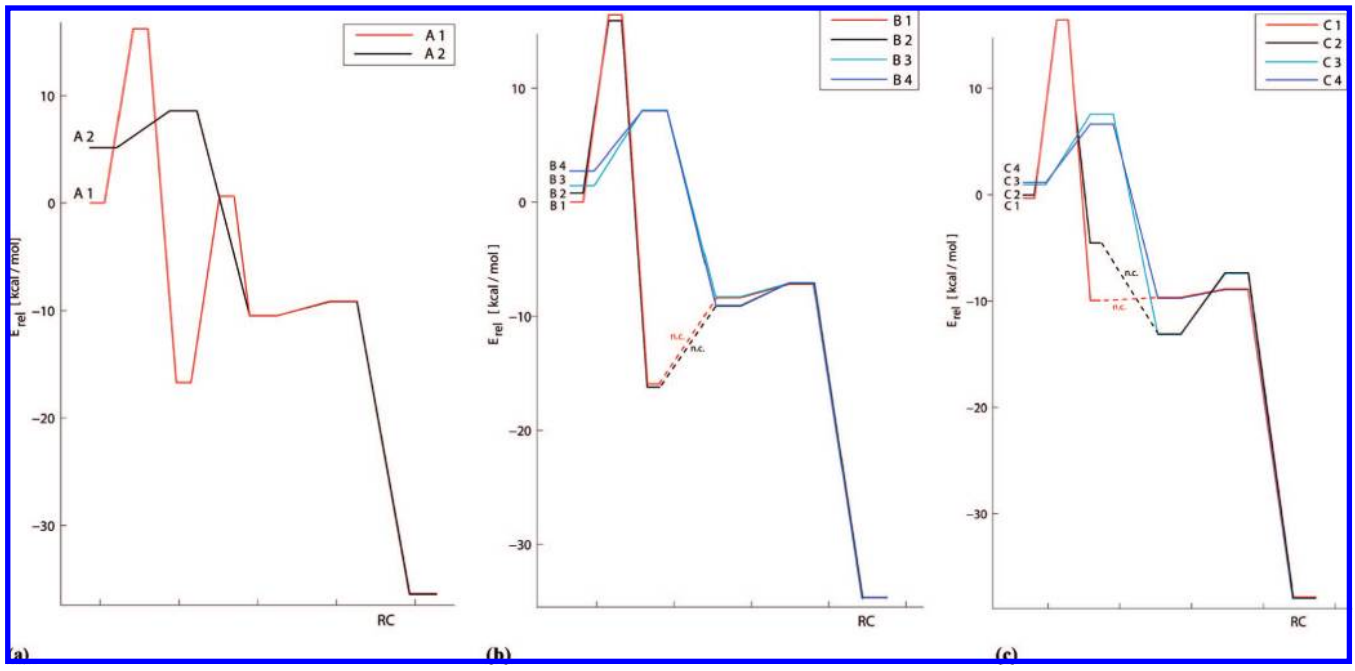

Figure 8. Summary of the reactions courses A1, A2, B1−B4, and C1−C4 for the addition of acetylene to 1,3-butadiene catalyzed by $[Co(L)]^+$.

only a summary of the calculated reaction coordinates for reactions C1−C4 in comparison with B1−B4 and with A1, A2.

It becomes obvious that the two-step processes A2, B3, B4, C3, and C4, which open with the higher-lying forms of the complex [Co(L)(1,3-butadiene)(acetylene)]$^+$, are clearly favored over the respective alternative reaction courses A1, B1, B2, C1, and C2. This is because the overall activation barriers of the rate-determining formation of the first C−C bond are lower for the two-step processes than for the three-step reactions, even when the energy differences between the isomeric forms of the starting complex [Co(L)(1,3-butadiene)(acetylene)]$^+$ are considered. A common feature of the starting complexes in the reaction courses A2, B3, B4, C3, and C4 is that the interatomic distance between the carbon atoms of the acetylene and the 1,3-butadiene ligands, which yield the first C−C bond in the stepwise reaction, is clearly shorter (between 2.707 Å in B4 and 2.752 Å in C4) than in the alternative pathways A1, B1, B2, C1, and C2 (between 2.908 Å in C2 and 3.093 Å in A1). Inspection of the starting complexes [Co(L)(1,3-butadiene)(acetylene)]$^+$ in the reaction courses A2, B3, B4, C3, and C4 (see Figures 6, 7, and S1) reveals that the 1,3-butadiene ligand binds with a different orientation with respect to the ligand L and particularly to the acetylene ligand than in the starting complexes in the pathways A1, B1, B2, C1, and C2. In the former complexes, the 1,3-butadiene moiety and the acetylene ligand are oriented in such a way that the reacting species may approach each other in a similar way as in the uncatalyzed concerted reaction (cf. Figure 2). In the starting complexes of the three-step reaction courses A1, B1, B2, C1, and C2, the 1,3-butadiene is rotated by ∼90°, and the acetylene ligand approaches 1,3-butadiene "from the backside", which permits the formation of only one C−C bond. The resulting intermediate

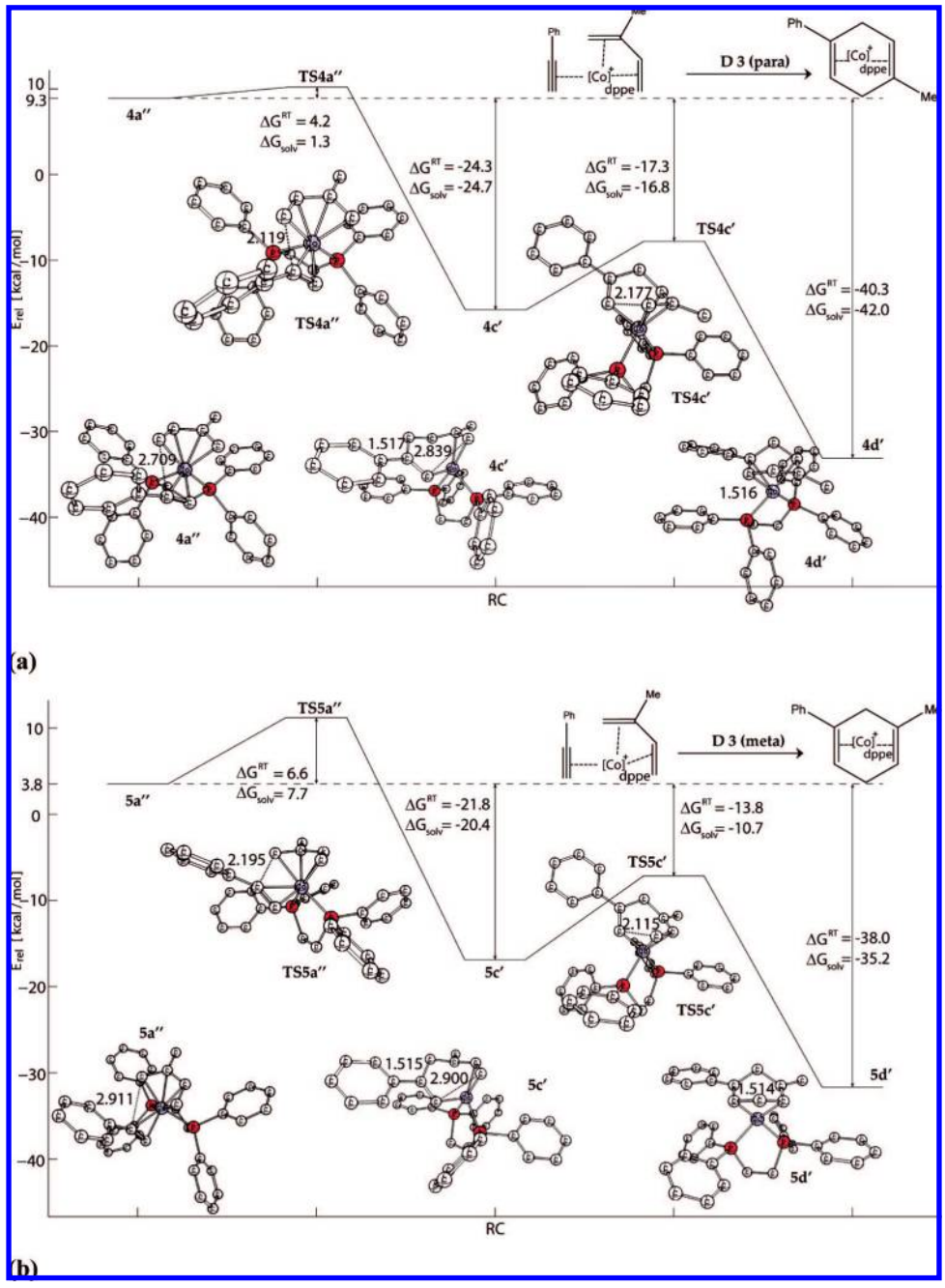

Figure 9. Kinetically most favorable reaction courses (a) D3(para) and (b) D3(meta) calculated at BP86/def2-SVP for the addition of phenylacetylene to isoprene, catalyzed by $[Co(dppe)]^+$, yielding the *para* and *meta* isomers. Free energy difference at 298 K (ΔG^{RT}) and after considering solvent effects of CH_2Cl_2 (ΔG_{solv}). The calculated interatomic distances are given in angstroms. Note that the reference value for the energies at 0 kcal/mol refers to the ΔG_{solv} scale. Hydrogen atoms are omitted for clarity.

complex must then rearrange before the second C−C bond can be formed. The starting complexes in A1, B1, B2, C1, and C2 are slightly lower in energy than the starting complexes in A2, B3, B4, C3, and C4, probably because of less steric crowding, but the latter structures are better suited for the C−C bond formation between acetylene and 1,3-butadiene because of the favorable orientation of the reacting species.

Cobalt-Catalyzed Reaction of Isoprene with Phenylacetylene: $[Co(dppe)]^+$. The results in the previous section showed that the $[Co(L)]^+$-catalyzed Diels−Alder reaction between the parent systems 1,3-butadiene and acetylene follows a stepwise rather than a concerted pathway and that there are several alternative reaction courses which need to be considered. It can be expected that the metal-catalyzed addition reaction between the substituted systems 2-methyl-1,3-butadiene (isoprene) and phenylacetylene (reactions 2a and 2b) leads to even more pathways starting from different complexes $[Co(L)(isoprene)(phenylacetylene)]^+$. Extensive calculations yielded, when L = dppe, four different reaction courses that lead to the *para* product and four pathways that lead to the *meta* product. For each regioisomer, there are two three-step pathways and two dual-step pathways. Figure 9 shows the kinetically most favorable reaction profiles, D3(para) and D3(meta), for the reaction of $[Co(dppe)(isoprene)(phenylacetylene)]^+$ yielding the *para* and *meta* products, respectively. The calculated reaction courses D1(para), D2(para), D4(para), D1(meta), D2(meta), and D4(meta) are shown in Figures S2 and S3 (Supporting Information).

The reaction courses D3(para) and D4(para) are two-step processes starting from the educt complexes **4a″** and **5a″** (Figure

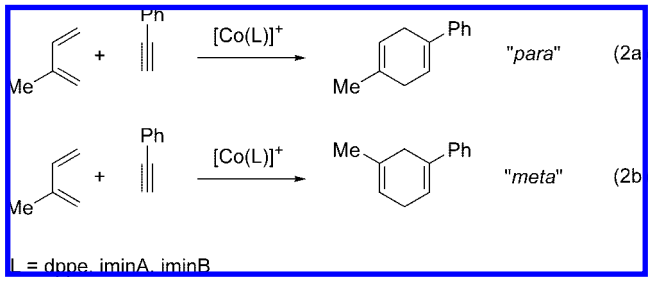

9). Note that the regioselectivity is determined in the first step of the reaction, where the initial C−C bond is formed, while the second step is not relevant for the regioselectivity of the product. The first reaction step is also rate-determining for the formation of the *para* and *meta* products. The free activation barriers, which include the relative energy of the starting complex with regard to the most stable educt, are $\Delta G^{\ddagger}_{RT} = 11.5$ kcal/mol for the *para* product and $\Delta G^{\ddagger}_{RT} = 12.7$ kcal/mol for the *meta* product (Table 1). The solvent CH_2Cl_2 slightly lowers the activation energy, which becomes $\Delta G^{\ddagger}_{solv} = 10.6$ kcal/mol for D3(para) and $\Delta G^{\ddagger}_{solv} = 11.6$ kcal/mol for D3(meta). Table 1 shows that the activation barriers for the other reaction courses D1(para), D2(para), and D4(para) leading to the *para* product and D1(meta), D2(meta), and D4(meta) yielding the *meta* product are significantly higher. Note that the inclusion of the solvent effect leads in some cases to a decrease but in other cases, such as D1(para), to a significant increase of the calculated activation barriers. We analyzed the electronic structure of the calculated species in order to find an explanation for the peculiar solvent effect. There is no correlation between the change in the dipole moment of educts and transition states and the change in the calculated activation barriers. We think that the change in the local charge distribution between educt and transition state greatly influences the calculated solvent effect, which could be further analyzed by calculating the molecular electrostatic potentials. Such an investigation is beyond the scope of the present work.

Figure 10 schematically displays the calculated reaction profiles D1(para)−D4(para) and D1(meta)−D4(meta) for the addition of phenylacetylene to isoprene, catalyzed by $[Co(dppe)]^+$. We want to point out that the pathways that have the lowest activation energies, D3(para) and D3(meta), do *not* start from the energetically lowest-lying educt conformation! The results demonstrate that it is important to investigate the conformational profiles of the reacting molecules in order to find the lowest-lying transition state.

Table 1 summarizes the calculated activation energies of the selectivity- and rate-determining first steps of reaction 2 with L = dppe. It becomes obvious that the inclusion of temperature and entropy contributions and the estimate of the solvent effect significantly influences the theoretical value for the regioselectivity. Table 2 gives the theoretically predicted and experimentally observed regioselectivities for the Diels−Alder reactions of isoprene with phenylacetylene, catalyzed by $[Co(L)]^+$ (L = dppe, iminA, iminB). The calculated value of $\Delta\Delta G^{\ddagger}_{solv} = 0.9$ kcal/mol for the most favorable pathways, D3(para) and D3(meta), in favor of the *para* product, gives a theoretically predicted ratio of 17.9:82.1 for the *meta*:*para* selectivity of reaction 2 (L = dppe). A Boltzman distribution over the eight activation barriers $\Delta\Delta G^{\ddagger}_{solv}$ gives a slightly different theoretical value of *meta*:*para* = 16.8:83.2. This is in excellent agreement with the experimental value of *meta*:*para* = 15:85 which has been reported by Hilt and co-workers.[10]

Cobalt-Catalyzed Reaction of Isoprene with Phenylacetylene: $[Co(iminA)]^+$. Calculations of the reaction profile for reaction 2 with L = iminA gave four pathways, E1(para)−E4(para), that lead to the *para* product and four pathways, E1(meta)−E4(meta), that lead to the *meta* product. All of them are two-step pathways where the C−C bonds are formed in a consecutive fashion. Figure 11 shows the kinetically most favorable pathways, E1(para) and E1(meta), which lead to the *para* and *meta* product, respectively. In both reaction courses, it is the terminal carbon atom of phenylacetylene that forms the first C−C bond. The calculated reaction courses D2(para)−D4(para) and D2(meta)−D4(meta) are shown in Figures S4 and S5 (Supporting Information).

Table 1 shows that the calculated effective activation energies for the first step of the most favorable reactions, which include the relative energies of the starting complexes with respect to the lowest-energy structure **7a**, are $\Delta G^{\ddagger}_{RT} = 9.5$ kcal/mol for E1(para) and $\Delta G^{\ddagger}_{RT} = 8.2$ kcal/mol for E1(meta). The calculated solvent effect on the former activation barriers changes the barriers only slightly. The reaction course E1(para) is unchanged after calculating the influence of CH_2Cl_2 on the energy of the kinetically most favorable pathway for formation of the *para* product ($\Delta G^{\ddagger}_{solv} = 8.9$ kcal/mol), but the pathway E3(para) has a slightly higher barrier ($\Delta G^{\ddagger}_{solv} = 9.3$ kcal/mol). The activation barrier for the first step of the reaction course E1(meta) is reduced to $\Delta G^{\ddagger}_{solv} = 5.9$ kcal/mol, which is clearly lower than the activation barriers for E1(para) and E3(para).[20]

Figure 12 schematically displays the calculated reaction profiles for the intramolecular addition reaction of $[Co(iminA)(isoprene)(phenylacetylene)]^+$, yielding the *meta* and *para* products. Table 1 shows that the formation of the *meta* product via pathway E1(meta) is kinetically slightly favored ($\Delta G^{\ddagger}_{RT} = 8.2$ kcal/mol) over the formation of the *para* product via the most favorable pathway E1(para) ($\Delta G^{\ddagger}_{RT} = 9.5$ kcal/mol). The energy difference between the activation barriers, $\Delta\Delta G^{\ddagger}_{RT} = 1.3$ kcal/mol, significantly increases in favor of the *meta* product to $\Delta\Delta G^{\ddagger}_{solv} = 3.0$ kcal/mol when the effect of the solvent CH_2Cl_2 is considered. Table 1 summarizes the activation energies of the first reaction step for the eight pathways. Table 2 shows that the calculated energy difference between the most favorable pathways that yield the *meta* and *para* products, $\Delta\Delta G^{\ddagger}_{solv} = 3.0$ kcal/mol, corresponds to a theoretical value for the ratio *meta*:*para* of 99.4:0.6, which does not change when the other pathways are considered. The theoretical value is in perfect agreement with the experimentally observed regioselectivity, *meta*:*para* = 99:1.[10]

Cobalt-Catalyzed Reaction of Isoprene with Phenylacetylene: $[Co(iminB)]^+$. We also calculated the reaction profiles for the addition of phenylacetylene to isoprene, catalyzed by $[Co(iminB)]^+$ (reaction 2). The results were similar to the data for the $[Co(iminA)]^+$-catalyzed reaction presented in the previous section. The calculations gave four pathways, F1(para)−F4(para), that lead to the *para* product and four pathways, F1(meta)−F4(meta), that lead to the *meta* product. Figures S2 and S3 show the theoretically predicted reaction pathways and the calculated equilibrium structures and transition states. Figure 13 gives an overview of the theoretically predicted energy profiles.

The calculations indicate that the four *para* pathways F1(para)−F4(para) and the four *meta* pathways F1(meta)−F4(meta) are two-step processes with consecutive formation of the two C−C bonds. The activation barrier for formation of the first carbon−carbon bond is the rate-determining step. Table 1 gives the calculated activation barriers for the eight processes. The lowest-energy pathway that leads to the *para* product is F1(para), which has an activation barrier of $\Delta G^{\ddagger}_{RT} = 8.2$ kcal/mol. The most favorable pathway leading to the *meta* product is F1(meta), which has a slightly lower barrier of $\Delta G^{\ddagger}_{RT} = 7.1$ kcal/mol. The PCM calculations, which consider the effect of CH_2Cl_2 as a solvent, considerably increase the energy difference in favor of the formation of the *meta* product, and they suggest that the reaction pathway F4(meta) rather than F1(meta) has the lowest activation barrier. The calculated lowest activation energies are $\Delta G^{\ddagger}_{solv} = 9.2$ kcal/mol for the *meta* product and $\Delta G^{\ddagger}_{solv} = 11.8$ kcal/mol for the *para* product. The difference between these values, $\Delta\Delta G^{\ddagger}_{solv} = 2.6$ kcal/mol, gives a theoretical ratio of *meta*:*para* = 98.8:1.2 for the $[Co(iminB)]^+$-catalyzed reaction 2, which is in excellent agreement with the experimentally observed regioselectivity *meta*:*para* = 95:5 (Table 2).[10] The calculations which include the other eight pathways do not alter the theoretically predicted *meta*:*para* ratio.

Table 1. Calculated (BP86/def2-SVP) Activation Energies (kcal/mol) for the Addition of Phenylacetylene to Isoprene, Yielding the *Para* and *Meta* Isomers, Catalyzed by $[Co(L)]^+$ (L = dppe, iminA, and iminB)[a]

reaction	$\Delta E^{\ddagger}$	$\Delta E^{\ddagger}_{ZPE}$	$\Delta G^{\ddagger}_{RT}$	$\Delta G^{\ddagger}_{solv}$	reaction	$\Delta E^{\ddagger}$	$\Delta E^{\ddagger}_{ZPE}$	$\Delta G^{\ddagger}_{RT}$	$\Delta G^{\ddagger}_{solv}$
				$[Co(dppe)]^+$					
D1 (para)	21.3	21.1	21.6	27.7	D1 (meta)	21.6	21.2	22.0	20.7
D2 (para)	19.2	18.6	18.8	19.4	D2 (meta)	17.6	17.3	17.9	17.2
D3 (para)	**11.4**	**11.2**	**11.5**	**10.6**	**D3 (meta)**	**12.7**	**12.2**	**12.7**	**11.6**
D4 (para)	17.2	17.0	17.5	16.4	D4 (meta)	15.9	15.5	16.1	15.9
				$[Co(iminA)]^+$					
E1 (para)	**7.8**	**8.1**	**9.5**	**8.9**	**E1 (meta)**	**6.7**	**7.1**	**8.2**	**5.9**
E2 (para)	10.1	10.0	10.8	10.9	E2 (meta)	10.8	11.0	11.9	12.6
E3 (para)	8.4	8.8	10.1	9.3	E3 (meta)	12.1	12.1	13.6	12.2
E4 (para)	9.1	9.5	10.9	11.2	E4 (meta)	8.3	8.8	10.3	9.4
				$[Co(iminB)]^+$					
F1 (para)	**7.5**	**7.7**	**8.2**	**11.8**	**F1 (meta)**	**6.8**	**6.9**	**7.1**	10.7
F2 (para)	10.2	10.3	10.9	14.9	F2 (meta)	10.8	10.8	11.3	15.1
F3 (para)	8.7	9.1	9.8	14.6	F3 (meta)	12.6	12.7	13.8	14.1
F4 (para)	9.4	9.3	9.6	16.2	**F4 (meta)**	7.2	7.5	8.4	**9.2**

[a] Bold entries give the most favorable pathways.

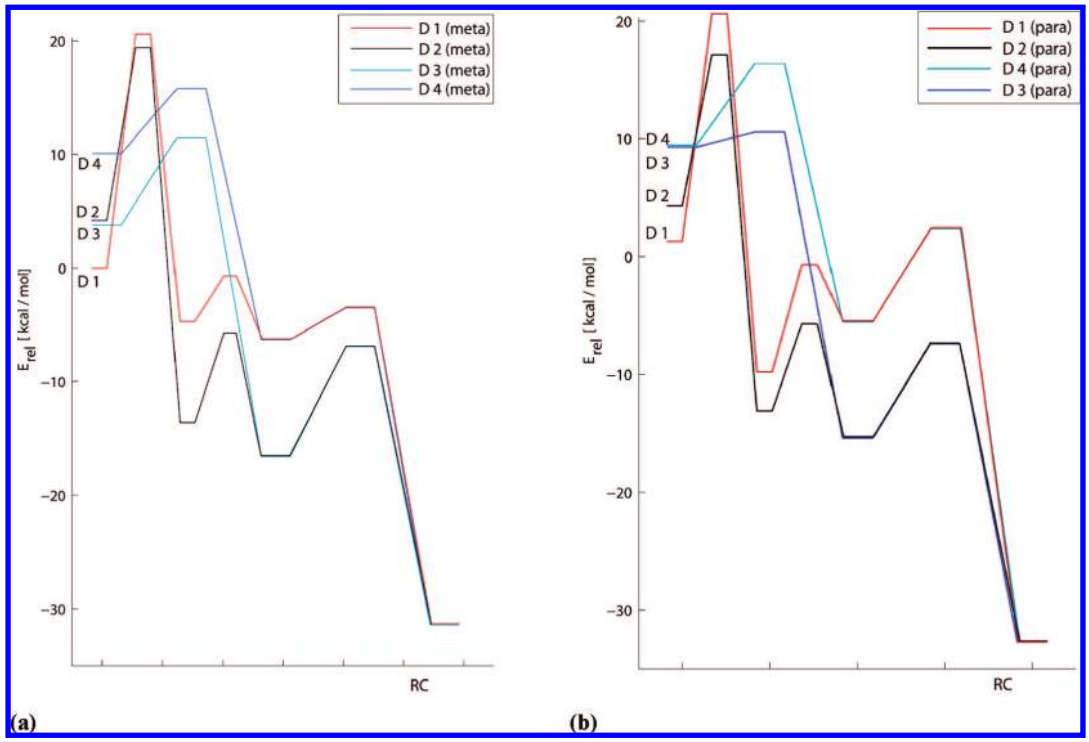

Figure 10. Summary of the reactions courses D1(para)−D4(para) and D1(meta)−D4(meta) for the addition of phenylacetylene to isoprene, catalyzed by $[Co(dppe)]^+$. (a) Three-step processes. (b) Two-step processes. The curves follow the ΔG^{RT} values.

Table 2. Calculated and Experimental Regioselectivities of the Cobalt-Catalyzed Addition of Phenylacetylene to Isoprene

catalyst	$\Delta\Delta G^{\ddagger}_{RT}$[a]	*meta*:*para*$_{RT}$[b]	$\Delta\Delta G^{\ddagger}_{solv}$[a]	*meta*:*para*$_{solv}$	*meta*:*para*$_{exptl}$
$[Co(dppe)]^+$	1.2	11.6:88.4 (11.5: 88.5)	0.9	17.9:82.1 (16.8: 83.2)	15:85
$[Co(iminA)]^+$	−1.3	90.0:10.0 (85.7: 14.3)	−3.0	99.4:0.6 (99.4: 0.6)	99:1
$[Co(iminB)]^+$	−0.9	82.1:17.9 (86.2: 13.7)	−2.6	98.8:1.2 (98.8: 1.2)	95:5

[a] Values in kcal/mol. A positive value indicates that the *para* product has a lower activation energy than the *meta* product. [b] The first value is calculated from the lowest activation energies yielding the *meta* and *para* product. The values in parentheses give the *meta*:*para* ratio calculated by considering the activation barriers of all eight reactions pathways.

The optimized transition states and intermediates for the $[Co(L)]^+$-catalyzed Diels−Alder reaction of isoprene with phenylacetylene suggest that the crucial steps of the reaction pathway are slightly different than in the anticipated catalytic cycle shown in Figure 4. There is no transition state for a concerted pathway. A new finding of the present work is that the stepwise formation of the 1,4-cyclohexadiene complex may involve a rearrangement of the metallacyclic compound generated in the first step.

Discussion

The results presented in the previous sections show that, after numerous reaction pathways with a large number of transition

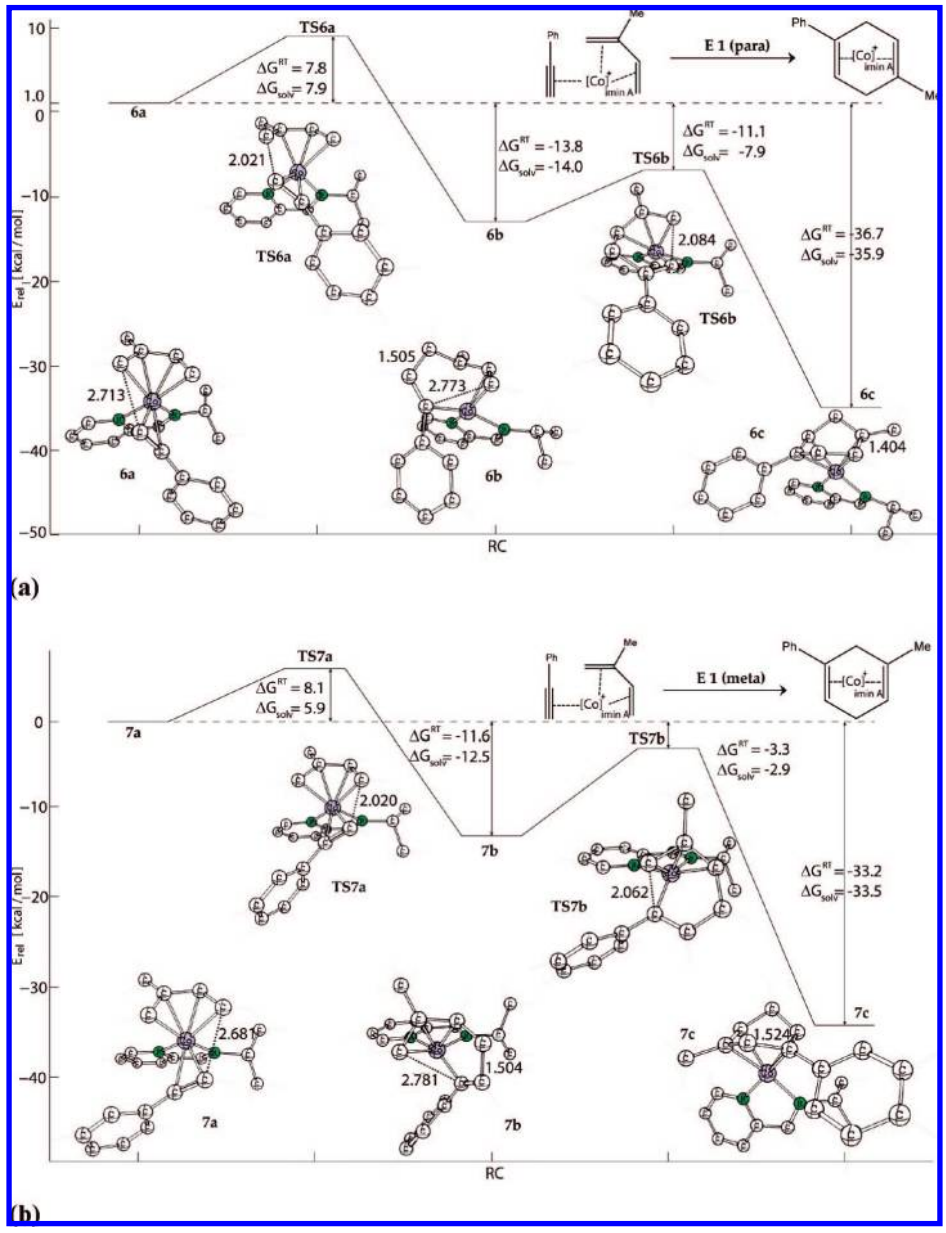

Figure 11. Kinetically most favorable reaction courses (a) E1(para) and (b) E1(meta) calculated at BP86/def2-SVP for the addition of phenylacetylene to isoprene, catalyzed by $[Co(iminA)]^+$, yielding the *para* and *meta* isomers. Free energy difference at 298 K (ΔG^{RT}) and after considering solvent effects of CH_2Cl_2 (ΔG_{solv}). The calculated interatomic distances are given in angstroms. Note that the reference value for the energies at 0 kcal/mol refers to the ΔG_{solv} scale. Hydrogen atoms are omitted for clarity.

states have been calculated, the theoretical values for the regioselectivities of the $[Co(L)]^+$-catalyzed Diels−Alder reaction of isoprene with phenylacetylene agree exceptionally well with the experimental values. Can any further insight be gained from the analysis of the theoretical data? The calculated results clearly demonstrate that it is not sufficient to consider the reaction pathways of the lowest-energy conformations of the starting complexes $[Co(L)(isoprene)(phenylacetylene)]^+$ for elucidating the factors that determine the stereoselectivity. Table 3 summarizes the energy differences ΔE of the latter species for L = dppe, iminA, and iminB and the calculated activation energies for formation of the first C−C bond $\Delta E^{\ddagger}$ with respect to the most stable conformation. It shows also which of the two possible C−C bonds are generated in the rate-determining step.

It becomes obvious that, in the $[Co(dppe)]^+$-catalyzed reaction that leads to the *para* product, the C4−C1′ bond is first generated in the kinetically most favorable pathway, D3(para), while in the lowest-energy pathway yielding the *meta* product, D3(meta), the C1−C1′ bond is the first carbon−carbon bond formed. Note that the order of C−C bond formation in D3(para) and D3(meta) does not agree with steric arguments of the reacting species, because the C−C bond between unsubstituted carbon atoms (C1−C2′ for the *para* product and C4−C2′ for

(20) One reviewer pointed out that the activation barrier for the second step of reaction course E1(meta) is higher ($\Delta G^{\ddagger}_{solv}$ = 8.9 kcal/mol) than for the first step, and therefore, the second step would be rate-determining. However, the regioselectivity is determined in the first step of the reaction. We postulate that there is no equilibrium between educts and intermediates because the activation barriers for the reverse reaction of the first step is much higher than the activation barrier of the second step. Thus, the stationary state approximation is not valid for the reaction courses presented here.

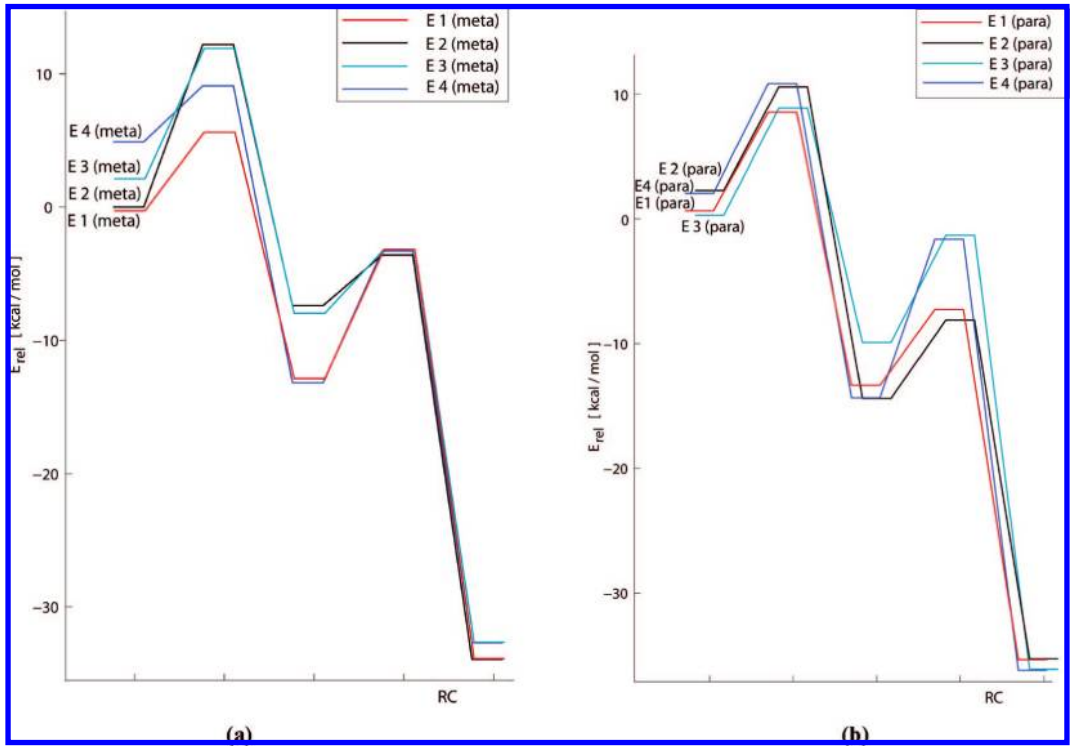

Figure 12. Summary of the reactions courses E1(para)−E4(para) and E1(meta)−E4(meta) for the addition of phenylacetylene to isoprene, catalyzed by $[Co(iminA)]^+$.

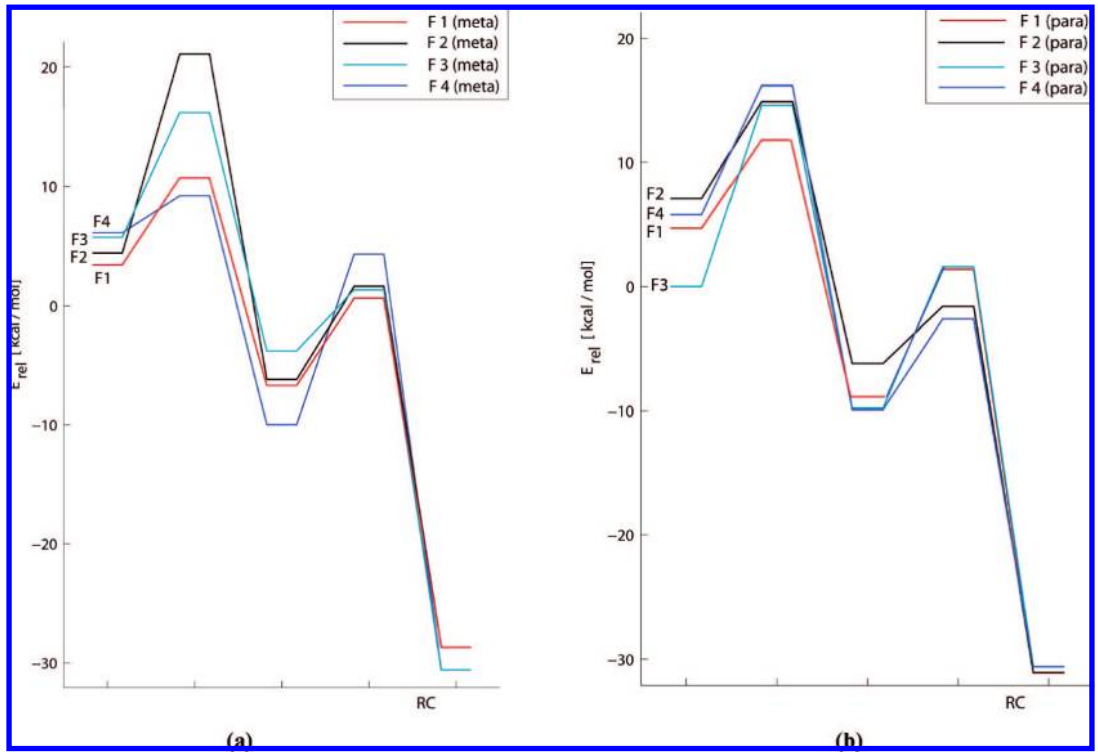

Figure 13. Summary of the reactions courses F1(para)−F4(para) and F1(meta)−F4(meta) for the addition of phenylacetylene to isoprene, catalyzed by $[Co(iminB)]^+$.

the *meta* product) is only closed in the final step. The order of bond formation is also not the same as in the concerted uncatalyzed reaction (Figure 2). The transition states for the latter reaction show that, in $\mathbf{TS_{para}}$, the formation of the C1−C2′ bond precedes the generation of the C4−C1′ bond, while in $\mathbf{TS_{meta}}$, the C4−C2′ bond is generated earlier than the C1−C1′ bond. The kinetically most favorable pathways, D3(para) and D3(meta), benefit from two factors which appear to be crucial for the activation energy: the distances between the terminal carbon atoms of the reacting species which lead to the new C−C bonds *and* the relative energy of the respective conformation. The shortest C−C distance of the starting complexes yielding

Table 3. Comparison of the Relative Energies (BP86/def2-SVP) of the Conformations for the Initially Formed Complexes ΔE with the Calculated Activation Energies with Respect to the Lowest-Energy Form $\Delta E^{\ddagger}$ (kcal/mol)[a]

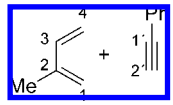

reaction	ΔE	$\Delta E^{\ddagger}$	C−C[b]	r(C−C)[c]	reaction	ΔE	$\Delta E^{\ddagger}$	C−C[b]	r(C−C)[c]
					[Co(dppe)]$^+$				
D1 (para)	0.0	21.3	1−2′	2.947	D1 (meta)	1.6	21.6	4−2′	3.038
D2 (para)	5.7	19.2	4−1′	3.153	D2 (meta)	4.0	17.6	1−1′	3.023
D3 (para)	**8.9**	**11.4**	**4−1′**	**2.709**	**D3 (meta)**	**6.7**	**12.7**	**1−1′**	**2.911**
D4 (para)	12.7	17.2	1−2′	2.669	D4 (meta)	9.6	15.9	4−2′	2.576
					[Co(iminA)]$^+$				
E1 (para)	**1.3**	**7.8**	**1−2′**	**2.713**	**E1 (meta)**	**0.2**	**6.7**	**4−2′**	**2.681**
E2 (para)	1.4	10.1	4−1′	2.898	E2 (meta)	0.0	10.8	1−1′	2.955
E3 (para)	0.6	8.4	1−2′	2.747	E3 (meta)	1.8	12.1	1−1′	2.970
E4 (para)	2.9	9.1	4−1′	2.904	E4 (meta)	4.6	8.3	4−2′	2.644
					[Co(iminB)]$^+$				
F1 (para)	**1.1**	**7.5**	**1−2′**	**2.719**	**F1 (meta)**	**0.6**	**6.8**	**4−2′**	**2.663**
F2 (para)	2.4	10.2	4−1′	2.895	F2 (meta)	1.3	10.8	1−1′	2.943
F3 (para)	0.0	8.7	1−2′	2.801	F3 (meta)	2.3	12.6	1−1′	2.941
F4 (para)	2.4	9.4	4−1′	2.901	F4 (meta)	2.9	7.2	4−2′	2.677

[a] Bold entries display the energetically lowest-lying pathways. [b] First C−C bond formed in the Diels−Alder reaction. [c] Distance between the carbon atoms in the starting complex.

the *para* product is calculated for reaction pathway D4(para) (2.669 Å), but the educt is the least stable conformation, 12.7 kcal/mol higher in energy than the starting complex of D1(para). The most favorable *para* reaction pathway, D3(para), has a slightly longer carbon−carbon distance in the starting complex (2.709 Å), and the educt is 8.9 kcal/mol less stable than the starting complex of D1(para). A similar situation is calculated for the reaction pathways yielding the *meta* product, where the kinetically most favorable pathway D3(meta) does not have the energetically most stable starting complex, nor does the latter possess the shortest carbon−carbon distance. We searched for electronic factors which might correlate with the regioselectivity of the reaction. Analysis of the orbital energies and orbital coefficients did not provide any clue because the frontier orbitals of the coordinated reacting partners strongly mix with the metal orbitals.

The data in Table 3 show that the most favorable pathways of the [Co(iminA)]$^+$- and [Co(iminB)]$^+$-catalyzed reactions exhibit the converse sequence of carbon−carbon bond formation compared with the [Co(dppe)]$^+$-catalyzed reaction. This holds for the reaction pathways leading to the *para* and *meta* products. The former reaction paths, E1(para) and F1(para), initiate with the formation of the C1−C2′ bond, while the reaction courses E1(meta) and F1(meta) start with the formation of the C4−C2′ bond. Note that the energy differences between the starting conformations of the [Co(iminA)]$^+$- and [Co(iminB)]$^+$-catalyzed reactions are much smaller than those of the [Co(dppe)]$^+$-catalyzed reactions. The most important factor that correlates with the lowest activation energy in the former two reactions is the carbon−carbon distance of the starting complex. The kinetically most favorable pathways, E1(para), F1(para), and F1(meta), have starting complexes which possess the shortest C−C distances of the emerging bonds. The interatomic C−C distance in the starting complex of the lowest-energy pathway, E1(meta) (2.681 Å), is slightly longer than that in E4(meta) (2.644 Å), but the latter species is 4.6 kcal/mol higher in energy than the former.

Experimental Test. The calculated results open the door for a rational design of [Co(L)]$^+$-catalyzed Diels−Alder reactions where the effect of ligands L on the regioselectivity of the addition of alkynes and dienes can be predicted with quantum chemical calculations and afterward tested with experimental investigations. As a first step, we examined the theoretical result concerning the influence of a polar solvent on the regioselectivity of the reaction of isoprene with phenylacetylene. Table 2 shows that the $\Delta\Delta G^{\ddagger}_{RT}$ values give a higher preference for the *para* product in the [Co(dppe)]$^+$-catalyzed reaction and a lower preference for the *meta* product in the [Co(iminA)]$^+$- and [Co(iminB)]$^+$-catalyzed reactions than the $\Delta\Delta G^{\ddagger}_{solv}$ values. This means that a less polar solvent should lead to a change in the *meta*:*para* ratio in the predicted direction. In order to verify the theoretical prediction, we carried out the [Co(L)]$^+$-catalyzed Diels−Alder reaction of isoprene with phenylacetylene in the same fashion as described by Hilt et al.,[10] but the polar solvent dichloromethane was replaced by the less polar solvent toluene. For these reactions, both catalysts Co(iminA) and Co(iminB) gave the cycloaddition product in a *meta*:*para* selectivity of 88:12, which means that the preference for the *meta* product is less than in the reactions with dichloromethane. The [Co(dppe)]$^+$-catalyzed reaction in toluene yielded a *meta*:*para* selectivity of 4:96, which is higher than in the reactions using dichloromethane. The experimental findings thus fully support the theoretical predictions.

Summary and Conclusion

The following conclusions can be drawn from this work.

• The [Co(L)]$^+$-catalyzed Diels−Alder reaction of isoprene with phenylacetylene takes place in a stepwise fashion, starting with the formation of the complex [Co(L)(isoprene)(phenylacetylene)]$^+$ as precursor for the consecutive C−C bond formation. The actual Diels−Alder ring-closing reaction proceeds as an intramolecular addition of the ligands isoprene and phenylacetylene, yielding a metallacyclic intermediate that is formed after generation of the first carbon−carbon bond, which is the rate-determining step.

• There are four different conformations of the starting complexes [Co(L)(isoprene)(phenylacetylene)]$^+$, which initiate four different pathways yielding the 1,3-cyclohexadiene product. It holds in all cases that the energetically most stable conformations do not lead to the reaction pathways with the lowest activation energies. All conformations and the associated pathways must be considered in order to obtain the kinetically most favorable reaction course.

• The calculated values for the regioselectivities of the [Co(L)]$^+$-catalyzed Diels−Alder reaction agree exceptionally well with the experimental values. The calculations concur with the experimental finding that the *para* product is kinetically favored for L = dppe, while the *meta* product is kinetically favored when L = iminA or iminB.

• The different regioselectivies for L = dppe and L = iminA or iminB come from (a) the steric interactions of the bidentate ligands with the isoprene and phenylacetylene moieties in [Co(L)(isoprene)(phenylacetylene)]$^+$, which determine the distance between the carbon atoms forming the C−C bond, and (b) the relative energies of the different starting complexes. The first C−C bond formed in the rate-determing step of the [Co(dppe)]$^+$-catalyzed reaction yielding the *para* product is the C4−C1′ bond, and for the *meta* product it is the C1−C1′ bond. The opposite order is found for the [Co(iminA)]$^+$- and [Co(iminB)]$^+$-catalyzed reactions, where the C1−C2′ bond forma-

tion is the initial step toward the *para* product, while the C4−C2′ bond is formed first in the reaction yielding the *meta* product.

• The calculations suggest that a less polar solvent should reduce the preference for formation of the *meta* product in the $[Co(iminA)]^+$- and $[Co(iminB)]^+$-catalyzed reactions and that it enhances the formation of the *para* product in the $[Co(dppe)]^+$-catalyzed reaction. Experimental tests using toluene instead of dichloromethane as solvent confirm the theoretical predictions.

Acknowledgment. This work is dedicated to Prof. R. W. Hoffmann on the occasion of his 75th birthday. This work was supported by the Deutsche Forschungsgemeinschaft. Excellent service by the Hochschulrechenzentrum of the Philipps-Universität Marburg is gratefully acknowledged. Further computer time was provided by the CSC Frankfurt, HLRS Stuttgart, and HHLRZ Darmstadt.

Supporting Information Available: Complete ref 12; Table S1, coordinates and energies of the calculated molecules; Figure S1, reaction courses C1−C4 for addition of acetylene to 1,3-butadiene catalyzed by $[Co(iminB)]^+$; Figure S2, reaction courses D1(para), D2(para), and D4(para) for addition of phenylacetylene to isoprene, catalyzed by $[Co(dppe)]^+$; Figure S3, reaction courses D1(meta), D2(meta), and D4(meta) for addition of phenylacetylene to isoprene, catalyzed by $[Co(dppe)]^+$; Figure S4, reaction courses E2(para)−E4(para) for addition of phenylacetylene to isoprene, catalyzed by $[Co(iminA)]^+$; Figure S5, reaction courses E2(meta)−E4(meta) for addition of phenylacetylene to isoprene, catalyzed by $[Co(iminA)]^+$; Figure S6, reaction courses F1(para)−F4(para) for addition of phenylacetylene to isoprene, catalyzed by $[Co(iminB)]^+$; Figure S7, reaction courses F1(meta)−F4(meta) for addition of phenylacetylene to isoprene, catalyzed by $[Co(iminB)]^+$. This material is available free of charge via the Internet at http://pubs.acs.org.

JA078242N